Structure/Property Relationships for Polyamide 6 / Organoclay Nanocomposites in the Melt and in the Solid State

Vitaly M. Karaman,[1] *Valery P. Privalko*,[1] *Eleonora G. Privalko*,*[1] *Bjorn Lehmann*,[2] *Klaus Friedrich*[2]

[1]Institute of Macromolecular Chemistry, National Academy of Sciences of Ukraine, 02160 Kyiv, Ukraine
E-mail: privalko@iptelecom.net.ua
[2]Institute for Composite Materials (IVW) Ltd, University of Kaiserslautern, D-67663 Kaiserslautern, Germany

Summary: Commercial nanocomposites of polyamide 6 prepared by melt compounding with organoclays were characterized by complex viscosities and relaxation time spectra derived from storage and loss shear moduli measured in the melt state at 230° C, and by wide- and small-angle X-ray scattering, differential scanning calorimetry and stretching calorimetry in the solid state.
In the melt state, the decrease of ~ 25 % (compared to the pristine sample) in Newtonian viscosity at the lowest clay loading (2.5 %) suggested a lower equilibrium elasticity modulus of an entangled melt, as the small amounts of organoclay nanoparticles acted as specific "diluents" for the initial entanglement network. However, by increasing the clay loading this effect disappeared due to the importance of strong interactions at the nanoparticle/melt interface, leading to the formation of a fairly thick boundary interphase (BI) around the nanoparticles and ending up in the build-up of an "infinite cluster" of clay nanoparticles coated with BI at the highest (albeit still unusually low) clay loading (7.5 %).
In the solid state, organoclay nanoparticles proved to induce the crystallographic $\alpha \rightarrow \gamma$ transformation of PA6 , while the matrix crystallinity in nanocomposites remained essentially unchanged. In the range of elastic (reversible) behavior below the apparent yield strains ϵ^* , the highest Young´s moduli E and the lowest linear thermal expansion coefficients α_L were observed for dried nanocomposites, while the lowest E and the highest α_L corresponded to the moisturized, pristine PA6. The endothermal process of shape distortion of the lamellar crystals was assumed to precede the onset of the exothermal process of lamellar fragmentation in the range of inelastic (irreversible) behaviour of PA6 above ϵ^* . The energy balance of the inelastic behaviour of nanocomposites was dominated by the endothermal process of lamellar shape distortion.

Keywords: boundary interphase; clay; nanocomposite; polyamide 6

 DOI: 10.1002/masy.200550309

Introduction

Idealized classical models assuming random distribution of isolated, spherical filler particles within a continuous, structureless polymer matrix [1] , invariably treated the filler volume fraction φ as the major factor controlling the properties of filled polymer composites. In the frame of such "pragmatic" models, the empirical observations of significant increase of, say, elasticity moduli and concomitant decrease of thermal expansivities of filled polymers, the smaller the particle size at the same filler loading, remained unexplained. Formally, this effect can be accounted for by a more realistic "physical" model which explicitly assumes the smearing-out of the "mathematical" (i.e., vanishingly thin) polymer/filler interface into a "boundary interphase" (BI) of quite appreciable thickness [2] . In this context, the contribution of BI to the properties of a polymer/filler composite will increase, leading to a higher total interfacial area (i.e., the smaller the filler particle size).

Apparently, these and similar observations prompted the development of polymer *nanocomposites* reinforced by relatively small amounts of ultrafine clay particles with at least one nano-size dimension and extremely high aspect ratios[3] . The processability of nanocomposites, however, can present some problems, in view of the extreme sensitivity of melt flow behaviour to the aspect ratio of clay nanoparticles [4] and to the quality of their dispersion (exfoliation)[4-7]. Viscoelastic studies of irradiation-grafted nano-inorganic particle-filled polypropylene composites in the melt state[8,9] revealed the onset of a plastic yield phenomenon for a nanocomposite with the filler volume content as low as 4.68 % . This was regarded as experimental evidence for the shear-resistant, infinite cluster of nanoparticles coated with a polymer boundary interphase (BI) when the ratio of the mean thickness of the polymer interlayer between neighbouring nanoparticles, $<L>$, to the mean radius of gyration of a polymer coil, $<R_g>$, approached the "critical" value, $<L>/<R_g> \approx 1$. Moreover, stretching calorimetry studies of these nanocomposites [10] revealed the considerable excess of Young's moduli concomitant to the deficit of thermal expansivities, limiting strains for elastic behavior and breaking strains compared to reasonable theoretical predictions. These results, combined with the X-ray data, were explained by the oriented, pre-stressed state of tie chains in the interlamellar space of the PP matrix.

In this contribution, similar experimental techniques were used to characterize the structure-property relationships for polyamide 6/organoclay nanocomposites in the melt and in the solid state.

Experimental

Materials

The pristine polyamide 6 (designated by the supplier as 200A) and three nanocomposites (299F, 299E and 299D) prepared by melt compounding of 200A with 2.5, 5.0 and 7.5 % , respectively, of organoclays (organically-treated mica-like clay platelets with very high aspect ratio; specific surface area 700 m^2/g) were supplied by RTP Co. (Winona, MN). Both as-received samples with moisture contents up to 2.5 % (series 1) and those evacuated at 393 K overnight to constant weight (series 2) were studied to check for the effects of humidity.

Techniques

Storage $G'(\omega)$ and loss $G''(\omega)$ shear moduli were measured with the PIRSP-03 rheometer in the range of linear viscoelasticity (amplitudes of harmonic vibrations on the order of 1 %) at 230° C in an angular frequency window spanning about three decades (ω = 10^{-2} to 10 rad/sec). The poor thermal stability of 200A prohibited measurements at higher temperatures.

Wide-angle X-ray scattering (WAXS) patterns in the range of scattering angles (2θ) from 5 to 40 deg were measured with a DRON-2,0 diffractometer ; small-angle X-ray scattering (SAXS) data in the scattering angles range from 3' to 5 deg were obtained with the standard Kratky camera (KRM-type diffractometer) as described elsewhere [10].

Specific heat capacity c_p was determined (relative error of a single run about 3 %) with a custom-made differential calorimeter with diathermal shells in the temperature interval from 150 to 550 K (that is, up to 50 K above the apparent melting point of 500 K).

The mechanical work (W) and concomitant heat effects (Q) in the step-wise loading (stretching)/unloading (contraction) cycles were measured (with the estimated mean error below 2 %) at room temperature by using the stretching calorimeter described elsewhere [10]. In every experimental run, each specimen was stretched at a constant velocity q^+ (10% of the total specimen length per minute) to a predetermined strain ε_i , stored at fixed ε_i to the full completion of mechanical and thermal relaxations, and thereafter allowed to contract at the same velocity q^- to zero force.

Results and discussion

1. Melt state

Both for the pristine polymer (sample 200A) and for the nanocomposite with the lowest organoclay loading (sample 299F) the loss moduli $G''(\omega)$ were considerably higher than the storage moduli $G'(\omega)$; moreover, both $G''(\omega)$ and $G'(\omega)$ exhibited a smooth increase with frequency ω. In contrast, one could identify at least two frequency intervals with distinctly different behaviour for the nanocomposite with the highest organoclay loading (299D). In the range of lowest frequencies (i.e., at $\omega < 0.1$ sec^{-1}), both $G'(\omega)$ and $G''(\omega)$ turned out to have nearly identical magnitudes and to be only weakly frequency-dependent. At higher frequencies, $G'(\omega)$ and $G''(\omega)$ started to diverge and to exhibit a frequency dependence (although much weaker than that for the pristine polymer). These data may be considered [8,9] as experimental evidence for the existence of a spatial network of filler particles coated with a polymer boundary layer in the low-frequency range, and for its plastic yield at higher frequencies for sample 299D. As might have been expected, the viscoelastic behaviour of the sample 299E is intermediate between those for two other nanocomposites.

In principle, the occurrence of the yield phenomenon in molten polymer composites should be directly observable at exceedingly low frequencies ; otherwise, it can be associated with a non-zero intercept on the square-root plots of $G'(\varphi)$ vs. $G'(0)$, as follows from the modified Casson equation [11]:

$$\sigma(\varphi)^{1/2} = \sigma_y^{1/2} + a\,\sigma(0)^{1/2}, \qquad (1)$$

where $\sigma(0)$ and $\sigma(\varphi)$ are the shear stresses for the matrix and for the composite, respectively, σ_y is the yield stress, and a is the fitting constant. As can be seen from Figure 1, for nanocomposites with low filler loading the intercepts are negligibly small, whereas for sample 299D one derives $\sigma_y \approx 30$ Pa.

As could be inferred from the approximate constancy of the complex viscosity $|\eta^*| = [(G'/\omega)^2 + (G''/\omega)^2]^{1/2}$ over fairly broad frequency intervals, in the range of low frequencies the samples 200A and 299F behaved as Newtonian liquids. Unexpectedly, the values of $|\eta^*|$ for the latter sample turned out lower by nearly 25% as if the small amounts of organoclay nanoparticles acted as specific "diluents" for the initial entanglement network. In contrast, no evidence for the Newtonian flow could be detected for the nanocomposite

200D with the highest organoclay loading ; instead, the complex viscosity $|\eta^*|$ strongly increased, more markedly for lower frequency. This behaviour confirmed the occurrence of plastic yield of an infinite cluster of nanoparticles coated with BI, preceding the macroscopic melt flow. The 299E nanocomposite exhibited an intermediate behavior.

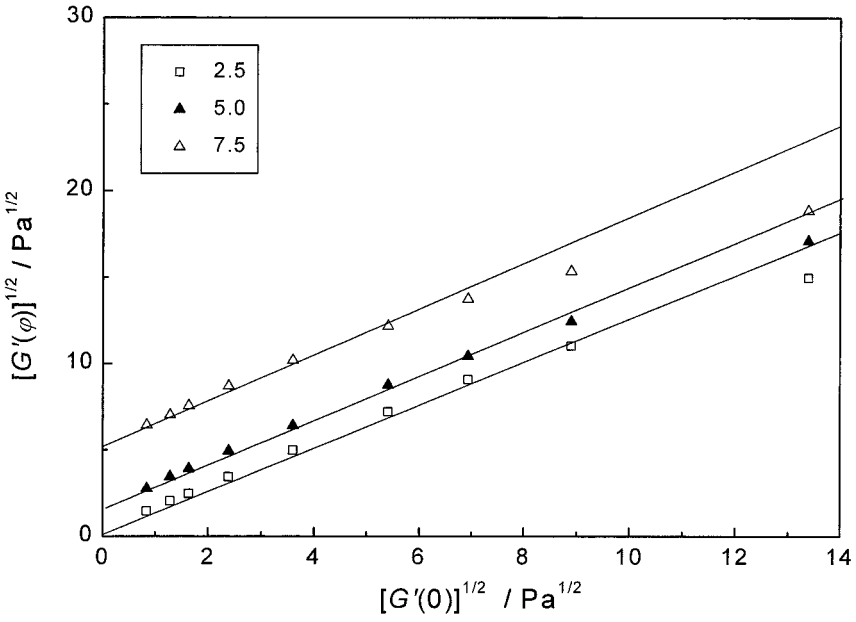

Figure 1. Modified Casson plots for nanocomposites with different organoclay loading.

2. Solid state

Reasonably strong WAXS reflections at the scattering vectors q = 14.4 and 16.4 nm^{-1} for the 200A nanocomposite (Figure 2a) were the evidence for predominance of monoclinic (α) crystal phase with hydrogen bonds between antiparallel chains in the pristine semi-crystalline PA6. These reflections could be also observed on the WAXS patterns of nanocomposites as shoulders flanking the main diffraction maximum at q = 15.0 nm^{-1}. The latter maximum and the subsidiary reflection at q = 7.5 nm^{-1} are characteristic for the pseudo-hexagonal (or monoclinic) crystal unit cell with hydrogen bonds between parallel chains (γ–modification) . The well-resolved SAXS reflection near $q \approx 0.62$ nm^{-1} (corresponding to the Bragg's periodicity $D \approx 10.1$ nm) for the 200A nanocomposite (Figure 2b) could not be resolved on

the SAXS curves of nanocomposites due to the increase of SAXS intensities in the same range of scattering vectors. These results suggested a significant increase of structural heterogeneity due to the appearance of new, strongly scattering entities (presumably, polymer-nanoparticle interfaces and microvoids) with a broad distribution of sizes.

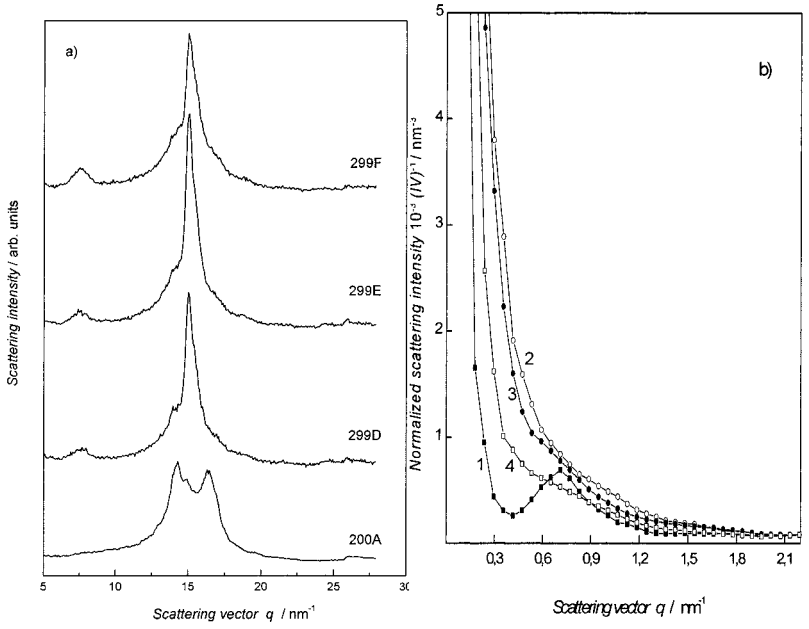

Figure 2. WAXS (a) and SAXS (b) patterns for 200 A (1), 299 D (2), 299 E (3) and 299 F (4).

In the range of elastic (reversible) deformations below a certain characteristic strain ε^* both the specific (per sample mass m) mechanical work (W/m) and specific heat effects (Q/m) data for all studied samples could be quantitatively fitted (Figure 3) to the classical equations of the thermoelasticity of solids [12]

$$W/m = E\varepsilon^2/2\rho \qquad (2a)$$

$$Q/m = E\alpha_L T\varepsilon/\rho \qquad (2b)$$

where E is the Young's modulus, α_L is the linear thermal expansion and ρ is the density. As expected, the best-fit values of E and α_L for moisture-plasticized samples of series 1 were systematically lower and higher, respectively, than those for corresponding dried samples of series 2. The observed overshoots of E, as well as the deficit of α_L for nanocomposites (Table

1) compared to theoretical predictions were regarded as experimental evidence for the oriented state of tie-chains in the interlamellar space of the PA matrix.

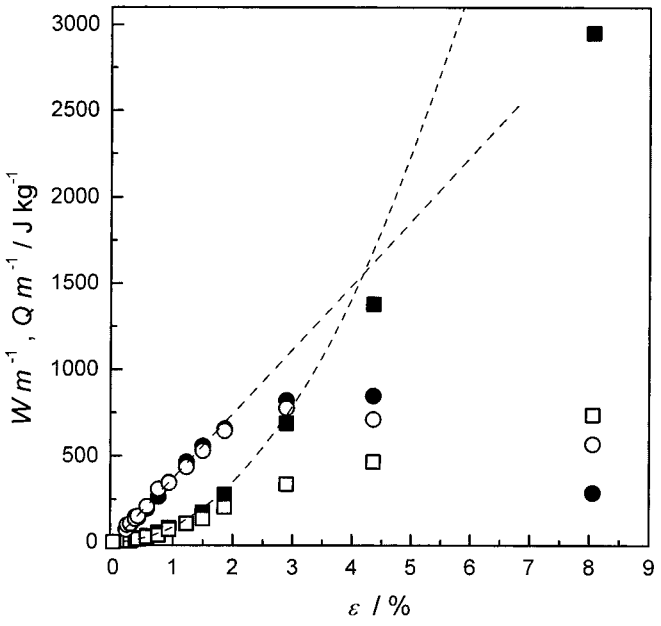

Figure 3. Specifi Figure 4. Specific internal energy increments for nanocomposites. Dashed line: theoretical curve for the hypothetical elastic behaviour of sample 200 A.

Table 1. Crystallinity (WAXS) and thermoelastic parameters for samples of series 1 and 2.

Sample	Clay content / %	X_{WAXS}	E / GPa	$10^4 \alpha_L$ / K^{-1}	ε^* / %	ε' / %	ε_b / %
200A	0	0.28/0.28	1.0/2.0	0.86/0.73	1.5/1.7	2.2/2.3	93/14.9
299D	7.5	0.34/0.38	1.6/2.7	0.80/0.60	1.3/1.4	2.2/2.0	11/3.9
299E	5.0	0.37/0.39	1.5/2.6	0.82/0.66	1.5/1.7	2.1/2.2	13/3.6
299F	2.5	0.30/0.29	1.3/2.4	0.87/0.71	1.7/1.8	2.3/2.2	23/1.8

The increasing differences between the values of W/m in stretching/contraction cycles above the apparent yield strains ε^* (Figure 3) are the evidence for the onset and subsequent development of irreversible (inelastic) structural changes within the polymer matrix (commonly referred to as plastic flow). Importantly, the deviations of experimental values of both W/m and Q/m in stretching regime from theoretical curves (dashed lines) set on at considerably higher strains ε' compared to ε^* . These data suggest the dominant contribution of a certain endothermal phenomenon into the mechanism of plastic flow of PA 6 in the strain interval $\varepsilon^* < \varepsilon < \varepsilon'$, while the contribution of the subsequent exothermal process responsible for the apparent deficit of Q/m becomes significant only above ε'. At this moment, the detailed mechanisms of the observed endothermal and exothermal phenomena remain unclear ; presumably, these may be attributed to successive processes of *shape distortion of the lamellar crystals* and of *lamellar fragmentation*, respectively [12]. In this context, the initial overshoot of W/m in stretching above that in contraction may be regarded as a measure of the specific mechanical energy irreversibly spent in the process of lamellar shape distortion.

The irreversible phenomena proved to set on at about the same apparent yield strains ε^* for the pristine polymer and for the nanocomposites. Formally, these data imply negligible (if any) contribution of *debonding* at the nanoparticle-matrix interface to the possible mechanisms of inelastic deformations. Additional check of this hypothesis can provide the analysis of specific internal energy increments, $\Delta U/m = (W + Q)/m$. As argued elsewhere [13], the deficit of $\Delta U/m$ in filled samples compared to that for the neat matrix polymer ($\delta(\Delta U/m) < 0$) would be considered as evidence for the heat released due to the formation of a free (debonded) filler surface. However, in contrast to the case of polyethylene/ kaolin composites [7] one observes the significant excess of $\Delta U/m$ with respect to the pristine PA6 (that is, $\delta(\Delta U/m) > 0$) for all nanocomposites (Figure 4). It can be thus concluded that of all possible mechanisms of irreversible structural rearrangements above ε^*, it is the endothermal process of lamellar shape distortion which dominates the energy balance of inelastic behaviour of nanocomposites.

Finally, smaller values of the breaking strains ε_b for nanocomposites compared to the pristine sample (Table 1) were attributed to the increased density of fibrillation and cavitation sites (presumably, localized at polymer/nanoparticle interfaces).

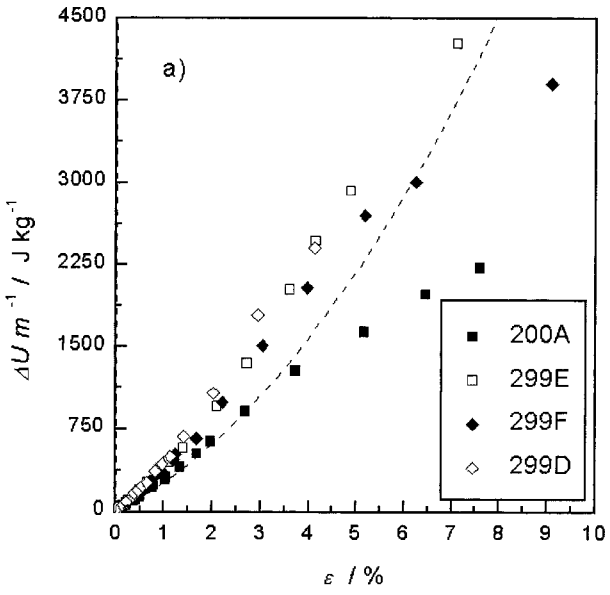

Figure 4. Specific internal energy increments for nanocomposites. Dashed line: theoretical curve for the hypothetical elastic behaviour of sample 200 A.

Conclusions

1. Strong interactions at the nanoparticle/melt interface are responsible for the formation of a fairly thick boundary interphase (BI) around the nanoparticles ending up in the build-up of an "infinite cluster" of clay nanoparticles coated with BI at the highest (albeit still unusually low) clay loading (7.5 %).

2. Organoclay nanoparticles induce crystallographic $\alpha \rightarrow \gamma$ transformation of PA6 , while the matrix crystallinity in nanocomposites remains essentially unchanged.

3. The endothermal process of shape distortion of the lamellar crystals is assumed to precede the onset of the exothermal process of lamellar fragmentation in the range of inelastic (irreversible) behaviour of PA6 above ε^* .

4. The energy balance of the inelastic behaviour of nanocomposites is dominated by the endothermal process of lamellar shape distortion

[1]. L.E. Nielsen, *"Mechanical Properties of Polymers and Composites"*, Marcel Dekker, Inc., New York 1974.
[2]. V.P. Privalko, V.V. Novikov, *"The Science of Heterogeneous Polymers"*, J. Wiley & Sons, Chichester, 1995.
[3]. Y. Fukushima, S. Inagaki, *J. Inclusion Phenom.* **1987**, *5*, 473-482.
[4]. K.H. Wang, M. Xu, Y.S. Choi, I.J. Chung, *Polymer Bull.* **2001**, *46*, 499-505.
[5]. E.P. Giannelis, *Adv. Mater.* **1996**, *8*, 29-35.
[6]. B. Hoffmann, J. Kressler, G. Stoeppelmann, C. Friedrich, G.M. Kim, *Colloid & Polymer Sci.* **2000**, *278*, 629-636.
[7]. Y.H. Hyun, S.T. Lim, H.J. Choi, M.S. Jhon, *Macromolecules* **2001**, *34*, 8084-8093.
[8]. V.F. Shumsky, E.G. Privalko, V.M. Karaman, V.P. Privalko, R. Walter, K. Friedrich, M.Q. Zhang, M.Z. Rong, *Adv. Compos. Let.* **2001**, *10*, 181-185.
[9]. V.P. Privalko, V.F. Shumsky, E.G. Privalko, V.M. Karaman, R. Walter, K. Friedrich, M.Q. Zhang, M.Z. Rong, *Sci. Technol. Adv. Mater.* **2002**, *3*,111-116.
[10]. V.P. Privalko, V.M. Karaman, E.G. Privalko, R. Walter, K. Friedrich, M.Q. Zhang, M.Z. Rong, *J. Macromol Sci. Phys.* **2002**, *41B*, 485-503.
[11]. M.M. Dumoulin, L.A.Utracki, P.J. Carreau, in: *"Two-Phase Polymer Systems"*, L.A. Utracki, Ed., Hanser Publ., Munich 1991, p. 185-212.
[12]. R.J. Young, *"Introduction to Polymers"*, Chapman and Hall 1989.
[13]. V.P. Privalko, F.J. Balta-Calleja, D.I. Sukhorukov, E.G. Privalko, R. Walter, K. Friedrich, *J. Mater. Sci.* **1999**, *34*, 497-508.